

2014

# Blocking the apoE/A $\beta$ interaction ameliorates A $\beta$ -related pathology in APOE $\epsilon$ 2 and $\epsilon$ 4 targeted replacement Alzheimer model mice

Joanna E. Pankiewicz  
*New York University School of Medicine*

Maitea Guridi  
*New York University School of Medicine*

Jungsu Kim  
*Washington University School of Medicine in St. Louis*

Ayodeji A. Asuni  
*New York University School of Medicine*

Sandrine Sanchez  
*New York University School of Medicine*

*See next page for additional authors*

Follow this and additional works at: [http://digitalcommons.wustl.edu/open\\_access\\_pubs](http://digitalcommons.wustl.edu/open_access_pubs)

---

## Recommended Citation

Pankiewicz, Joanna E.; Guridi, Maitea; Kim, Jungsu; Asuni, Ayodeji A.; Sanchez, Sandrine; Sullivan, Patrick M.; Holtzman, David M.; and Sadowski, Martin J., "Blocking the apoE/A $\beta$  interaction ameliorates A $\beta$ -related pathology in APOE  $\epsilon$ 2 and  $\epsilon$ 4 targeted replacement Alzheimer model mice." *Acta Neuropathologica Communications*.2,1. 75. (2014).  
[http://digitalcommons.wustl.edu/open\\_access\\_pubs/3098](http://digitalcommons.wustl.edu/open_access_pubs/3098)

---

**Authors**

Joanna E. Pankiewicz, Maitea Guridi, Jungsu Kim, Ayodeji A. Asuni, Sandrine Sanchez, Patrick M. Sullivan, David M. Holtzman, and Martin J. Sadowski

RESEARCH

Open Access

# Blocking the apoE/A $\beta$ interaction ameliorates A $\beta$ -related pathology in APOE $\epsilon$ 2 and $\epsilon$ 4 targeted replacement Alzheimer model mice

Joanna E Pankiewicz<sup>1,3</sup>, Maitea Guridi<sup>1</sup>, Jungsu Kim<sup>4,5,6,7</sup>, Ayodeji A Asuni<sup>1</sup>, Sandrine Sanchez<sup>1</sup>, Patrick M Sullivan<sup>8,9</sup>, David M Holtzman<sup>4,5,6</sup> and Martin J Sadowski<sup>1,2,3,10\*</sup>

## Abstract

Accumulation of  $\beta$ -amyloid (A $\beta$ ) in the brain is essential to Alzheimer's disease (AD) pathogenesis. Carriers of the apolipoprotein E (APOE)  $\epsilon$ 4 allele demonstrate greatly increased AD risk and enhanced brain A $\beta$  deposition. In contrast, APOE  $\epsilon$ 2 allele carriers show reduced AD risk, later age of disease onset, and lesser A $\beta$  accumulation. However, it remains elusive whether the apoE2 isoform exerts truly protective effect against A $\beta$  pathology or apoE2 plays deleterious role albeit less pronounced than the apoE4 isoform. Here, we characterized APP<sub>SW</sub>/PS1<sub>dE9</sub>/APOE  $\epsilon$ 2-TR (APP/E2) and APP<sub>SW</sub>/PS1<sub>dE9</sub>/APOE  $\epsilon$ 4-TR (APP/E4) mice, with targeted replacement (TR) of the murine ApoE for human  $\epsilon$ 2 or  $\epsilon$ 4 alleles, and used these models to investigate effects of pharmacological inhibition of the apoE/A $\beta$  interaction on A $\beta$  deposition and neuritic degeneration. APP/E2 and APP/E4 mice replicate differential effect of human apoE isoforms on A $\beta$  pathology with APP/E4 mice showing a several-fold greater load of A $\beta$  plaques, insoluble brain A $\beta$  levels, A $\beta$  oligomers, and density of neuritic plaques than APP/E2 mice. Furthermore, APP/E4 mice, but not APP/E2 mice, exhibit memory impairment on object recognition and radial arm maze tests. Between the age of 6 and 10 months APP/E2 and APP/E4 mice received treatment with A $\beta$ 12-28P, a non-toxic, synthetic peptide homologous to the apoE binding motif within the A $\beta$  sequence, which competitively blocks the apoE/A $\beta$  interaction. In both lines, the treatment significantly reduced brain A $\beta$  accumulation, co-accumulation of apoE within A $\beta$  plaques, and neuritic degeneration, and prevented memory deficit in APP/E4 mice. These results indicate that both apoE2 and apoE4 isoforms contribute to A $\beta$  deposition and future therapies targeting the apoE/A $\beta$  interaction could produce favorable outcome in APOE  $\epsilon$ 2 and  $\epsilon$ 4 allele carriers.

**Keywords:** Apolipoprotein E, Alzheimer's disease,  $\beta$ -amyloid, Neurodegeneration, Therapy

## Introduction

Alzheimer's disease (AD) is a familial and sporadic neurodegenerative disease. Its neuropathological hallmarks include parenchymal plaques and vascular deposits of  $\beta$ -amyloid (A $\beta$ ), intraneuronal paired helical filaments composed of hyperphosphorylated tau and ubiquitin, widespread loss of synapses and neurons, and the appearance of reactive astrocytes and microglia. Converging lines of evidence derived from genetic, neuropathological,

biomarker, and transgenic animal studies implicate disturbance of A $\beta$  homeostasis leading to its progressive accumulation in the brain as a driving mechanism of AD pathogenesis (reviewed in [1,2]). A $\beta$  is a 39- to 43-residue-long hydrophobic peptide, which readily self-aggregates into synaptotoxic oligomers and thioflavin-S (Th-S)-binding fibrils. Mutations in amyloid precursor protein (APP) or presenilin (PS) 1 and 2 genes found in familial AD cases increase total A $\beta$  secretion or alter a ratio of A $\beta$ <sub>1-40</sub>:A $\beta$ <sub>1-42</sub> production, resulting in increased secretion of the more toxic and aggregation-prone A $\beta$ <sub>1-42</sub> [1]. In the far more prevalent sporadic AD, the mechanism(s) underlying disturbance of A $\beta$  homeostasis are less obvious, but inheritance of the apolipoprotein (apo) E isoforms has been thus far established by numerous independent studies

\* Correspondence: sadowm01@med.nyu.edu

<sup>1</sup>Department of Neurology, New York University School of Medicine, New York, NY 10016, USA

<sup>2</sup>Department of Psychiatry, New York University School of Medicine, New York, NY 10016, USA

Full list of author information is available at the end of the article

as the strongest genetic factor modulating overall risk of occurrence of the disease and age of onset (reviewed in [3]). ApoE is a 34-kDa lipid carrier protein, which in the brain is produced by astrocytes and secreted as nascent, high-density lipoprotein-like particles [4]. Three major isoforms of apoE are encountered in humans, differing by the occurrence of cysteine and arginine in positions 112 and 158: apoE2 (Cys112, Cys158), apoE3 (Cys112, Arg158), and apoE4 (Arg112, Arg158). These single-amino-acid variations in the apoE sequence have serious effects on its properties, with apoE2 having reduced binding affinity for the low density lipoprotein (LDL) receptor [5] and apoE4 exhibiting an intrinsic domain interaction that alters its lipid-binding properties and results in an increased risk of hyperlipidemia and atherosclerosis [4]. Inheritance of the APOE  $\epsilon$ 4 allele is the strongest known risk factor for sporadic AD and shows direct association with increased A $\beta$  plaque load and reduced age of disease onset [6-8]. Conversely, the APOE  $\epsilon$ 2 allele appears to delay, and reduce the relative risk of developing AD and is associated with a lower burden of A $\beta$  deposits compared with the most common APOE  $\epsilon$ 3 allele [9,10]. To provide a mechanistic explanation for the variable effect of apoE isoforms on A $\beta$  accumulation and overall disease risk, it has been proposed that they produce a differential effect on A $\beta$  clearance and A $\beta$  aggregation and deposition [3]. However, it remains unclear whether the effect of apoE2 on A $\beta$  pathology is truly protective, or whether apoE2 merely plays deleterious role albeit less pronounced than that of apoE4. To exert its promoting effect on A $\beta$  aggregation and brain deposition, apoE directly interacts with A $\beta$ , binding to its amino-acid residues 12-28 [11,12]. In this study, we analyzed long-term outcomes of the pharmacological disruption of the apoE/A $\beta$  interaction in the background of apoE2 or apoE4, which show differential effect on A $\beta$  pathology and AD morbidity. For this purpose we used APP<sub>SW</sub>/PS1<sub>ΔE9</sub> AD transgenic (Tg) model mice with targeted replacement (TR) of both murine Apoe alleles with the human APOE  $\epsilon$ 2 or APOE  $\epsilon$ 4 alleles, which continued to be expressed under the control of the endogenous mouse Apoe promoter [13]. As previously shown, human APOE alleles targeted to APP<sub>SW</sub>/PS1<sub>ΔE9</sub> mice reproduce their differential effect on the magnitude of A $\beta$  plaque load [13] but do not delay onset of A $\beta$  deposition compared to APP<sub>SW</sub>/PS1<sub>ΔE9</sub> mice expressing native murine apoE [14]. Since these APP<sub>SW</sub>/PS1<sub>ΔE9</sub>/APOE  $\epsilon$ 2-TR and APP<sub>SW</sub>/PS1<sub>ΔE9</sub>/APOE  $\epsilon$ 4-TR lines (hereafter designated as APP/E2 and APP/E4; respectively) are novel AD Tg animal models, their behavioral and biochemical characterization was undertaken as a part of this study. To pharmacologically disrupt the apoE/A $\beta$  interaction, we used a previously characterized non-toxic, synthetic peptide A $\beta$ 12-28P, which is

homologous to the apoE binding motif within the A $\beta$  sequence [12,13,15]. In A $\beta$ 12-28P, proline replaces valine in the 18 position and the peptide was synthesized with D-amino acids and end-protected for extended serum half-life and increased BBB permeability [12]. A $\beta$ 12-28P inhibits apoE4/A $\beta$  binding with  $K_i = 12.9$  nM and neutralizes the promoting effect of apoE on A $\beta$  fibrillization *in vitro*, but has no effect on self-assembly of A $\beta$  in the absence of apoE [15]. Therefore, this study also evaluated the prospects for disrupting the apoE/A $\beta$  interaction in human population diversified by the occurrence of various APOE alleles.

## Material and methods

### Materials and reagents

Unless stated otherwise all reagents and antibodies were purchased from Sigma-Aldrich (St. Louis, MO). A $\beta$ 12-28P, A $\beta$ <sub>1-40</sub>, and A $\beta$ <sub>1-42</sub> peptides were custom synthesized and purified in the WM Keck Proteomic Facility of Yale University (New Haven, CT) in the laboratory of Dr. James I. Elliott as previously described [12,13].

### Animals

All mouse care and experimental procedures were approved by Institutional Animal Care and Use Committees of the New York University School of Medicine and the Washington University School of Medicine. APP/E2 and APP/E4 mice were generated by crossing-breeding of APP<sub>SW</sub>/PS1<sub>ΔE9</sub> mice [14] with APOE  $\epsilon$ 2-TR or APOE  $\epsilon$ 4-TR mice [16,17] as previously described [13]. APOE  $\epsilon$ 2-TR or APOE  $\epsilon$ 4-TR mice retain regulatory sequences of the mouse Apoe gene and the noncoding murine exon 1 surrounding the inserted human exons 2', 3', and 4' [17,18] and therefore, they express the human apoE protein at physiological levels. Both lines were maintained by mating APP/E2 and APP/E4 founders with APOE  $\epsilon$ 2-TR and APOE  $\epsilon$ 4-TR animals, respectively. Husbandry and genotyping was performed as previously described [13]. Mice were maintained in a barrier facility with a 12/12-h light/dark cycle and ad libitum food and water access. Female APP/E2 and APP/E4 mice received treatment with vehicle or A $\beta$ 12-28P from the age of 6 to 10 months. A $\beta$ 12-28P was diluted to 2 mg/mL in sterile phosphate buffered saline at pH 7.4 directly before injections and intraperitoneally administered three times a week (0.8 mg per injection). Vehicle treated mice received injections with phosphate buffered saline only. Immediately prior to concluding the study the animals were subjected to behavioral testing conducted following our published protocols [15,19,20]. Age and sex-matched littermates of APP/E2 and APP/E4 mice in which genotyping was negative for the APP<sub>SW</sub>/PS1<sub>ΔE9</sub> transgene (hereafter designated as WT/E2 and WT/E4, respectively) were used as an apoE isoform background control during

the behavioral and serological testing. After concluding the experiment, all animals were killed with an overdose of sodium pentobarbital (150 mg/kg). The blood was collected through a cardiac puncture and the serum was separated by centrifugation. Animals were transcardially perfused and their brains and internal organs collected for histopathological analysis as previously described [15].

#### **Histological processing, immunohistochemistry, and unbiased morphometric analysis**

Series of 40  $\mu\text{m}$ -thick serial brain sections evenly spaced every 400  $\mu\text{m}$  along the entire rostral-caudal brain axis were stained with Th-S to visualize fibrillar A $\beta$  deposits, with Gallyas silver stain to identify plaque-associated neuritic dystrophy [21], or immunohistochemically with monoclonal antibody (mAb) HJ3.4 raised against the N-terminus of A $\beta$  (1:250) [13] or with mAb 3D12 (1:200) raised against apoE (Novus Biologicals; Littleton, CO). The intensity of HJ3.4 and 3D12 immunostaining was enhanced by 10 min pretreatment with 44% formic acid (FA) and the immunohistochemistry protocol was concluded using 3,3'-diaminobenzidine and Cy3, respectively. The load of Th-S and 3D12 immunopositive amyloid plaques in the neocortex and hippocampus was determined using unbiased sampling and automated image threshold analysis, as previously described [13,15]. The density of neuritic plaques was calculated by counting their total number on all serial sections from a Gallyas stained series and then dividing the number obtained by the cumulative area of all the neocortical or hippocampal cross-sectional profiles.

#### **A $\beta$ ELISA**

Cortical mantle and hippocampi were dissected out, homogenized, and subjected to diethylamine (DEA) and FA extractions as previously described [15]. Concentrations of A $\beta$  peptides in DEA and FA brain extracts were determined by sandwich ELISAs using mAbs HJ2 and HJ7.4, which selectively discriminate between C-terminal configuration of A $\beta_{x-40}$  and A $\beta_{x-42}$ , respectively; as coating antibodies (1  $\mu\text{g}/\text{well}$ ) [13] and biotinylated mAb 4G8 (1:2,000) (Covance; Princeton, NJ) directed against A $\beta$  residues 17–24 as the detection antibody [22,23]. Since the N-terminal configuration of A $\beta$  peptides measured by ELISA remained uncharacterized we referred to them as A $\beta_{x-40}$  and A $\beta_{x-42}$ . ELISA readouts were converted to actual peptide concentrations based on readouts from standard curves prepared from FA-treated synthetic A $\beta_{1-40}$  and A $\beta_{1-42}$  peptides and multiplied by all dilutions made during DEA and FA extractions. Final values of brain concentrations of A $\beta$  peptides were reported in reference to the total brain protein concentration, the latter determined in a neat brain homogenate using the bicinchoninic acid assay (Pierce Biotechnology Inc.;

Rockford, IL). The concentration of A $\beta$  oligomers was determined in the neat homogenate using a human aggregated  $\beta$ -amyloid ELISA kit (Invitrogen, Carlsbad, CA) [13].

#### **ApoE ELISA**

Sandwich ELISA for apoE was performed using mAb 3D12 (1:2,000) as the capture antibody and biotinylated goat anti-human apoE polyclonal antibody (1:2,500) (Meridian Life Science, Inc.; Memphis, TN) as the detection antibody. ApoE concentrations were quantified in DEA and FA brain extracts. ELISA readouts were converted to apoE concentrations using standard curves prepared from recombinant human apoE2 or apoE4 (Leinco Technologies, Inc., St. Louis, MO) and multiplied by all dilutions made during DEA or FA extractions. The final brain apoE concentrations were reported in reference to the total brain protein concentration.

#### **Statistical analysis**

RAM data were analyzed using one-way analysis of variance (ANOVA) followed by the Newman-Keuls post hoc test. All other data sets were compared using the unpaired Student's *t* test with Welch's correction following confirmation of normal data distribution by the Kolmogorov-Smirnov and Shapiro-Wilk tests. All statistical analyses were performed using GraphPad Prism v5.04 (GraphPad Software, Inc., La Jolla, CA).

## **Results**

#### **Treatment of APP/E2 and APP/E4 mice with A $\beta$ 12-28P**

Female APP/E2 and APP/E4 mice received A $\beta$ 12-28P or vehicle through intraperitoneal injections from the age of 6 to 10 months. The treatment commenced at the start of A $\beta$  plaque formation in these Tg lines. Veterinary staff closely monitored the animals undergoing treatment for any signs of toxicity. Monitoring parameters included body weight, physical appearance, changes in coat appearance, occurrence of unprovoked behavior, and blunted or exaggerated responses to external stimuli. APP/E2 and APP/E4 mice receiving vehicle and A $\beta$ 12-28P showed no differences in respect to those parameters compared to their WT/E2 and WT/E4 age and sex-matched littermates, respectively. Measurements of the immune response against A $\beta$  in post-treatment sera of APP/E2 and APP/E4 mice showed no evidence of increased titer of anti-A $\beta$  antibodies in IgG and IgM classes associated with A $\beta$ 12-28P treatment (Additional file 1: Figure S1A and B). This observation indicates that treatment outcomes of A $\beta$ 12-28P administration cannot be accounted for by an anti-A $\beta$  vaccination effect.



### Effect of A $\beta$ 12-28P treatment on serum cholesterol and apoE levels

We also monitored the effect of A $\beta$ 12-28P treatment on the serum cholesterol and apoE levels. Ten-month-old APP/E2 mice showed a 5.1-fold higher total serum cholesterol level and a 13.2-fold higher serum apoE level than APP/E4 mice ( $p < 0.001$ ) (Additional file 1: Figure S2A). These findings are consistent with type III hyperlipoproteinemia, previously described in human APOE  $\epsilon$ 2-T $\epsilon$ R mice [17]. Compared to the vehicle control mice, A $\beta$ 12-28P treatment was associated with a reduction of the total serum cholesterol level by 15.7% in APP/E2 animals and by 33.3% in APP/E4 animals ( $p < 0.05$ ) (Additional file 1: Figure S2A). In addition, the total serum apoE level showed a mild but insignificant reduction with A $\beta$ 12-28P treatment in both APP/E2 and APP/E4 mice (Additional file 1: Figure S2B). Consistently with our previously published observations [15] these results indicate that A $\beta$ 12-28P exerts an effect on serum cholesterol metabolism in addition to targeting the apoE/A $\beta$  interaction in the brain.

### Behavioral studies

The performance of vehicle- and A $\beta$ 12-28P-treated APP/E2 and APP/E4 mice was compared to those of sex and age matched WT/E2 and WT/E4 littermates, which received no treatment. Behavioral testing included the object recognition test (ORT), which tests animals' long-term recognition memory, followed by the radial arm maze (RAM), which is a test of animals' spatial working memory. Behavioral studies were conducted during the last 3 weeks of the treatment experiment and during the testing mice continued to receive vehicle or A $\beta$ 12-28P injections. During the acquisition session of the ORT, when the animals are allowed to explore freely the two identical objects presented in the testing arena, WT/E2, and vehicle- and A $\beta$ 12-28P-treated APP/E2 mice, equally interacted with both objects as expected of normal mice (data not shown). Following a 3-h interval, which the mice spent in their home cages, one of the two familiar objects was replaced with a novel one, and the behavior of the mice was then observed during the retention session. All three tested mice groups spent significantly more time exploring the novel object than the familiar one during the retention session (Figure 1A), consistent with normal rodent exploratory behavior. WT/E4 mice, and vehicle- and A $\beta$ 12-28P-treated APP/E4 mice, also interacted equally with two identical objects during the ORT acquisition session (data not shown). However, during the retention session, WT/E4 mice and A $\beta$ 12-28P-treated APP/E4 mice spent significantly more time exploring the novel object, while vehicle-treated APP/E4 mice failed to demonstrate significant preference toward the novel object (Figure 1B).

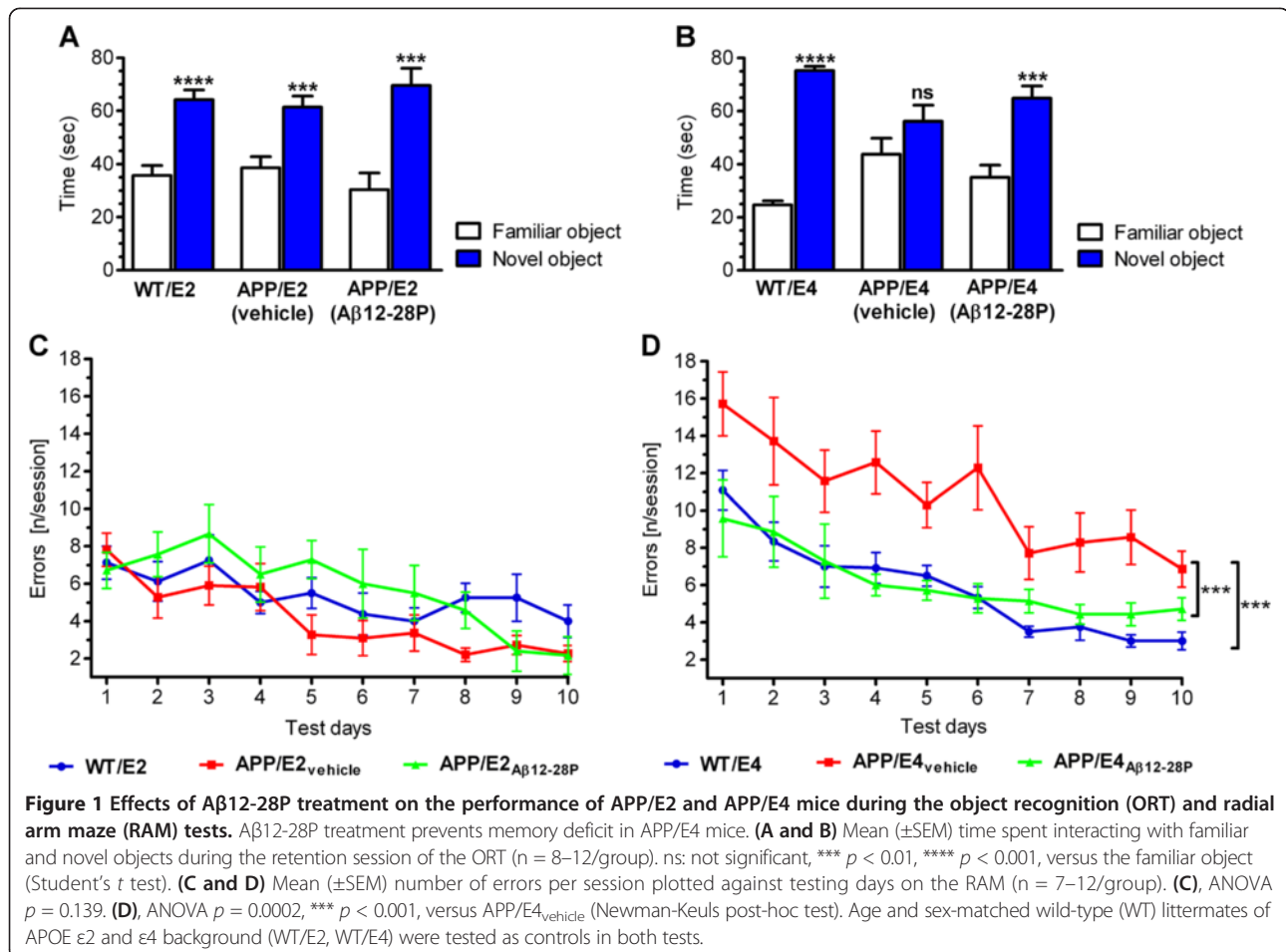
During RAM testing, WT/E2 mice, and vehicle- and A $\beta$ 12-28P-treated APP/E2 mice showed gradual improvement in performance on consecutive testing days, making comparable number of errors while navigating through the maze (Figure 1C). WT/E4 mice and vehicle- and A $\beta$ 12-28P-treated APP/E4 mice also showed gradual improvement in performance on consecutive days of RAM testing. However, vehicle-treated APP/E4 mice made significantly more errors than WT/E4 mice ( $p < 0.001$ ) and A $\beta$ 12-28P-treated APP/E4 mice ( $p < 0.001$ ), confirming the presence of memory impairment in APP/E4 mice at the age of 10 months (Figure 1D). A $\beta$ 12-28P-treated APP/E4 mice showed no significant difference from WT/E4 mice in the RAM testing, indicative of a therapeutic effect of apoE4/A $\beta$  binding disruption *in vivo*.

### Analysis of A $\beta$ plaque load

The load of Th-S positive A $\beta$  plaques (percentage of cross-sectional area of an anatomical structure covered by the plaques) was quantified in the neocortex and the hippocampus on serial coronal brain sections. In vehicle-treated APP/E4 mice, the load of Th-S-stained plaques in the neocortex and the hippocampus was 2.6- and 2.9-fold higher than that in APP/E2 mice ( $p < 0.0001$ ), (Figure 2A and B). A $\beta$ 12-28P treatment was associated with reduction of A $\beta$  plaque load in the neocortex and the hippocampus in APP/E2 mice by 41.7% ( $p < 0.001$ ) and 34.4% ( $p < 0.05$ ), respectively, while in APP/E4 mice the reduction was 23.0% ( $p < 0.01$ ) and 21.7% ( $p < 0.05$ ), respectively. As Th-S reveals only fibrillar structure of A $\beta$  plaques, we also stained serial brain sections with mAb HJ3.4 directed against the N-terminus of A $\beta$  [13,24]. Differences in the load of A $\beta$  plaque deposits shown by anti-A $\beta$  immunohistochemistry among APP/E2 and APP/E4 mice treated with vehicle or A $\beta$ 12-28P corresponded to that revealed by Th-S staining (Figure 2C). A small number of A $\beta$  deposits associated with brain and meningeal vessels was also seen in APP/E4 mice, however, their appearance was too sparse and variable from one brain section to the next to be reliably quantified.

### Biochemical analysis of brain A $\beta$ levels

Brain A $\beta_{x-40}$  and A $\beta_{x-42}$  levels (please see The Methods section for explanation of A $\beta$  peptide nomenclature used here) were measured following DEA and formic acid FA extractions, which release soluble A $\beta$  and insoluble A $\beta$  associated with A $\beta$  plaques and vascular deposits, respectively. Striking differences between vehicle-treated APP/E2 and APP/E4 mice were noted. In APP/E4 mice, soluble A $\beta_{x-40}$  and A $\beta_{x-42}$  levels were 7.7-fold and 22.5-fold higher than those in APP/E2 mice ( $p < 0.0001$ ), respectively; while insoluble A $\beta_{x-40}$  and A $\beta_{x-42}$  levels were 5.6-fold ( $p < 0.001$ ) and 9.2-fold ( $p < 0.01$ ) higher than those in APP/E2 mice, respectively (Figure 3A-D). Furthermore, the two lines



significantly differed in the A $\beta_{x-40}$ :A $\beta_{x-42}$  ratio. In APP/E2 mice the level of soluble A $\beta_{x-40}$  was 2.1-fold higher than that of soluble A $\beta_{x-42}$  ( $p < 0.0001$ ), while in the APP/E4 mice the opposite relation was observed, with the level of soluble A $\beta_{x-42}$  being 1.4-fold higher than that of soluble A $\beta_{x-40}$  ( $p < 0.05$ ). In APP/E2 mice, levels of insoluble A $\beta_{x-40}$  and A $\beta_{x-42}$  were similar, while in APP/E4 mice the level of insoluble A $\beta_{x-42}$  was 1.8-fold higher than that of A $\beta_{x-40}$  ( $p < 0.05$ ). In both APP/E2 and APP/E4 mice, insoluble A $\beta_{x-40}$  and A $\beta_{x-42}$  levels were over 15-fold higher than those of soluble peptides ( $p < 0.001$ ).

A $\beta$ 12-28P treatment was associated with a significant reduction in levels of soluble A $\beta_{x-40}$  and A $\beta_{x-42}$ , which in APP/E2 mice were reduced by 30.1% ( $p < 0.001$ ) and 35.8% ( $p < 0.0001$ ), respectively; while in APP/E4 mice by 32.1% ( $p < 0.05$ ) and 38.2% ( $p < 0.01$ ), respectively (Figure 3A and B). Levels of insoluble A $\beta_{x-40}$  and A $\beta_{x-42}$  in A $\beta$ 12-28P-treated APP/E2 mice were reduced by 44.2% and 51.8%, respectively ( $p < 0.0001$ ); while in A $\beta$ 12-28P-treated APP/E4 mice by 30.6% and 33.8%, respectively ( $p < 0.05$ ) (Figure 3C and D). Furthermore, we measured the brains' content of A $\beta$  oligomers using ELISA, which utilizes the same mAb as both the capture and detection

antibody, allowing four-member solid phase sandwiches to be formed only when aggregates containing multiple A $\beta$  copies are present in the sample. As with other forms of A $\beta$ , the concentration of A $\beta$  oligomers in vehicle-treated APP/E4 mice was 79.2-fold higher than that in APP/E2 mice ( $p < 0.001$ ). A $\beta$ 12-28P treatment reduced the level of A $\beta$  oligomers by 46.1% and 23.5% in APP/E2 and APP/E4 mice, respectively ( $p < 0.001$ ) (Figure 3E).

#### Analysis of the brain apoE level and its accumulation within A $\beta$ plaques

Levels of soluble and insoluble human apoE were measured in brain homogenate extracted with DEA and FA, respectively. There was no significant difference in the level of soluble apoE between vehicle-treated APP/E2 and APP/E4 mice (Figure 4A). The insoluble apoE level was 2-fold higher in APP/E4 mice than in APP/E2 mice ( $p < 0.0001$ ) (Figure 4B). A $\beta$ 12-28P treatment was associated with a 34.1% ( $p < 0.01$ ) reduction in the soluble apoE level in APP/E2 mice and a 45.7% reduction in the level in APP/E4 mice ( $p < 0.0001$ ). Insoluble apoE levels were reduced with A $\beta$ 12-28P treatment by 41.4% in APP/E2 mice ( $p < 0.0001$ ) and by 54.6% in APP/E4 mice ( $p < 0.0001$ ).

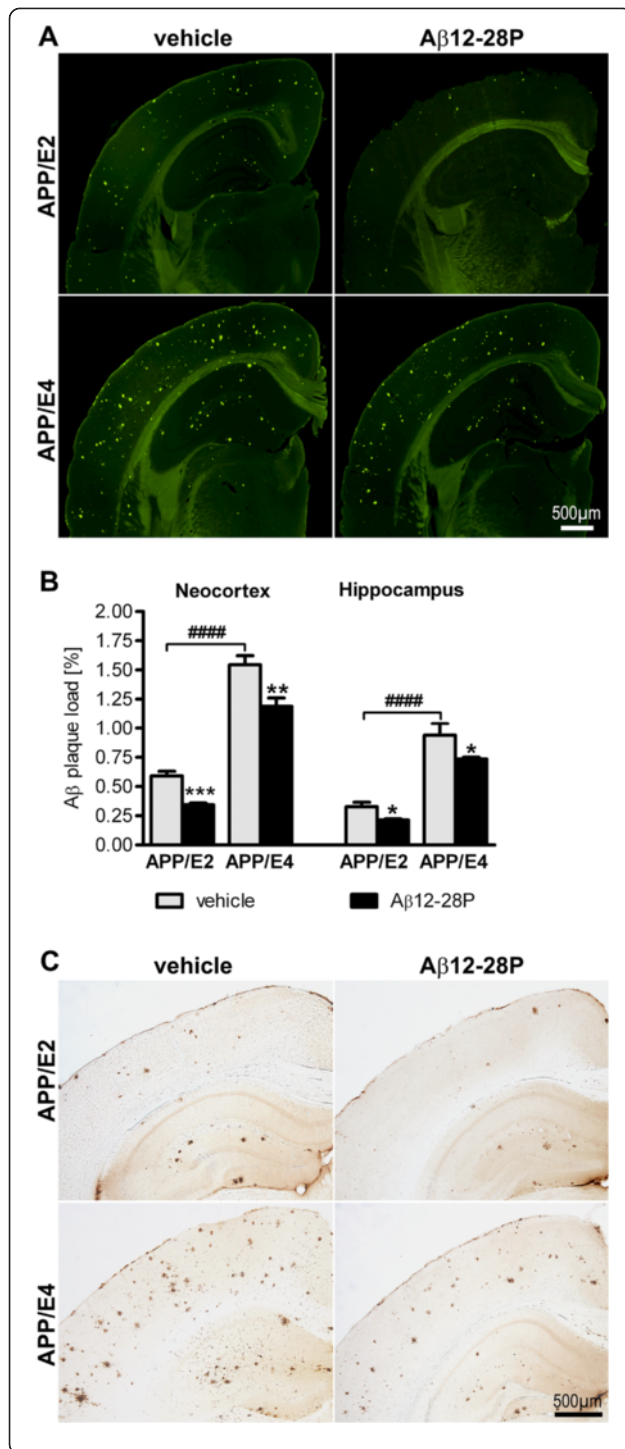


**Figure 2 Analysis of Aβ plaque load.** Aβ12-28P treatment reduces Aβ plaque formation in the neocortex and hippocampus of APP/E2 and APP/E4 mice. **(A)** Representative microphotographs of thioflavin-S-stained coronal brain sections from vehicle- and Aβ12-28P-treated APP/E2 and APP/E4 mice at the level of the dorsal hippocampus. **(B)** Mean (±SEM) thioflavin-S positive Aβ plaque load in the neocortex and the hippocampus (n = 7–8/group). \*  $p < 0.05$ , \*\*  $p < 0.01$ , \*\*\*  $p < 0.001$ , vs. vehicle-treated mice of the same APOE background, (Student's *t* test). ####  $p < 0.0001$ , vehicle-treated APP/E2 mice vs. vehicle-treated APP/E4 mice (Student's *t* test). **(C)** Representative microphotographs of coronal brain sections from vehicle- and Aβ12-28P-treated APP/E2 and APP/E4 mice showing the hippocampus, and somatosensory cortex, which were immunostained against the N-terminus of Aβ. Scale bars 500 μm **(A and C)**.

Furthermore, we quantified the load of apoE-positive plaque load, which also bound the amyloid dye Th-S. The load of apoE plaques was 2.9-fold higher in the neocortex ( $p < 0.0001$ ) and 4.2-fold higher in the hippocampus ( $p < 0.01$ ) in vehicle-treated APP/E4 mice than in the corresponding structures of vehicle-treated APP/E2 mice (Figure 4C and D). Aβ12-28P treatment was associated with a 26.9% reduction in the apoE-positive plaque load in the neocortex ( $p < 0.05$ ) and a 37.5% reduction in the hippocampus ( $p < 0.05$ ) in APP/E2 mice, and with a 49.9% ( $p < 0.001$ ) and 48.5% ( $p < 0.05$ ) reduction in the corresponding structures in APP/E4 mice, respectively.

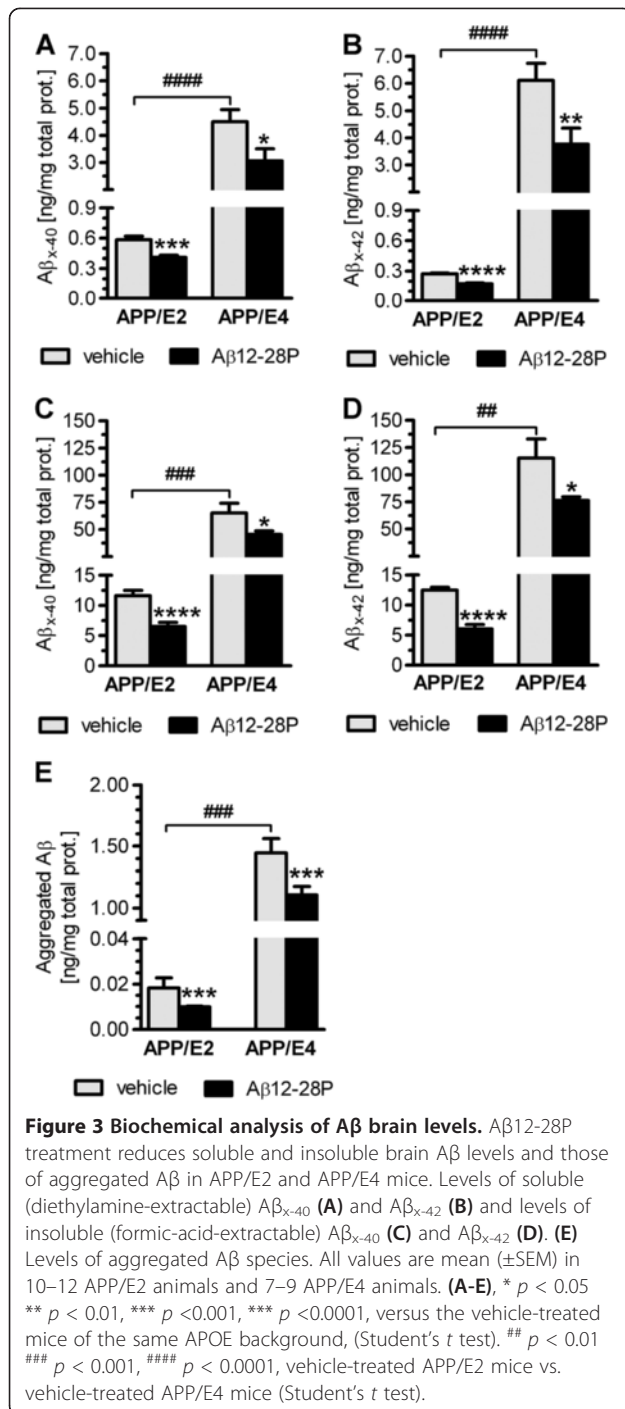
#### Neuritic plaques

Neuritic dystrophy associated with Aβ plaques was revealed using the Gallyas silver stain (Additional file 1: Figure S3 A-E). In APP/E4 mice, the numerical density of neuritic plaques in the neocortex and the hippocampus was 5.2-fold and 6.5-fold higher than those in the corresponding structures of APP/E2 mice, respectively ( $p < 0.001$ ) (Figure 5A and B). Aβ12-28P treatment reduced the neuritic plaques density in the neocortex and the hippocampus of APP/E2 mice by 47.1% and 38.5%, respectively ( $p < 0.05$ ), while in APP/E4 mice by 48.8% ( $p < 0.001$ ) and 43.6% ( $p < 0.01$ ), respectively.

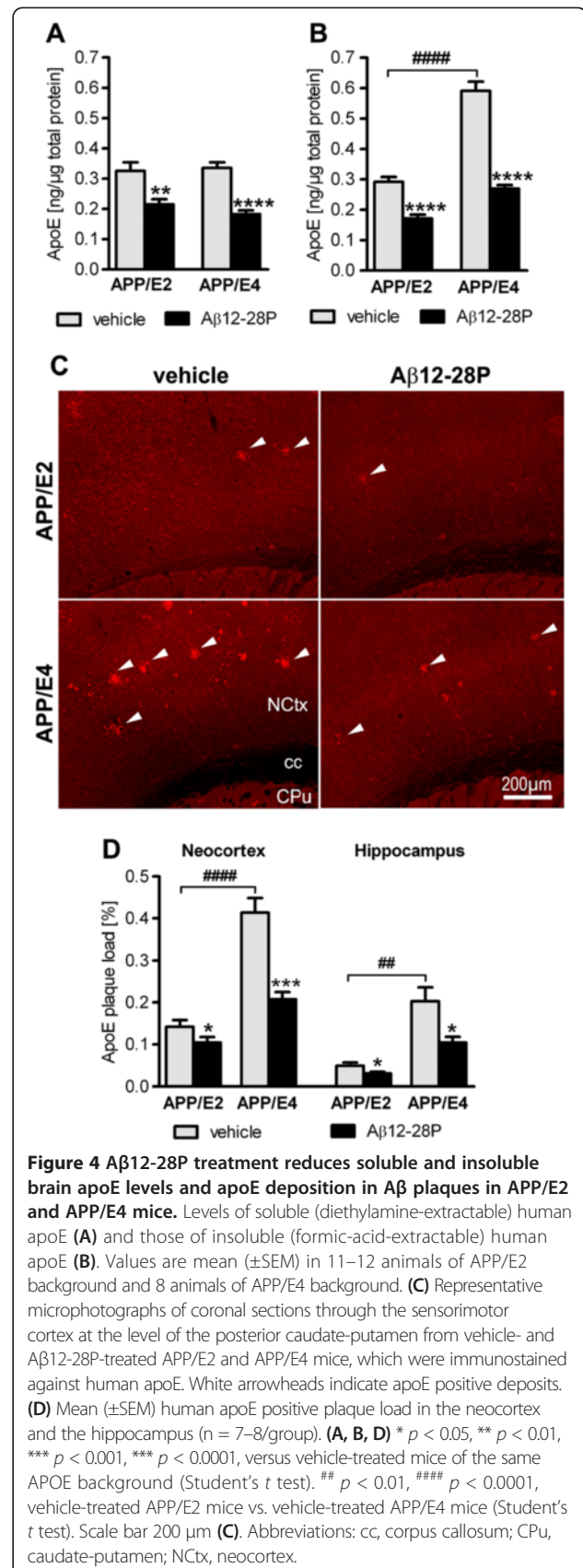
#### Discussion

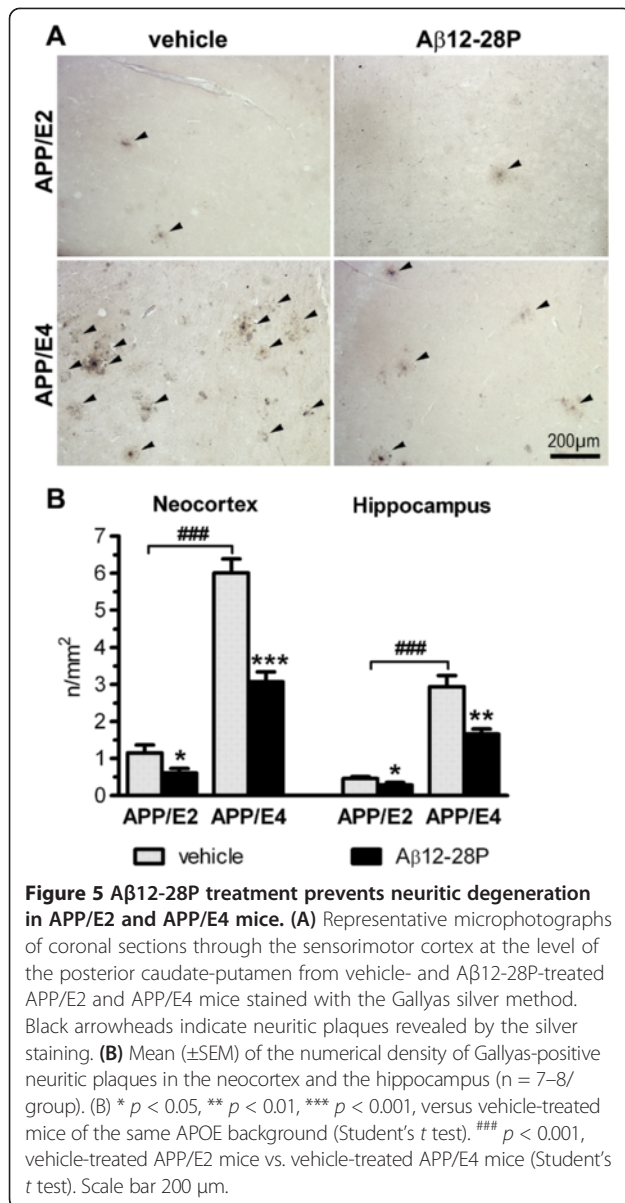
ApoE isoforms differentially modulate Aβ metabolism, Aβ accumulation, and AD morbidity in human subjects. We demonstrated here that APOE ε2 and APOE ε4 targeted replacement in APP<sub>SW</sub>/PS1<sub>ΔE9</sub> AD Tg model mice reproduces the differential effect of encoded by these alleles apoE isoforms on various aspects of Aβ pathology and associated neurodegeneration. Ten-month-old APP/E2 mice showed no behavioral deficit compared to WT/E2 mice, despite a modest Aβ plaque load and Aβ oligomer level. In contrast, age and sex matched APP/E4 mice revealed a pronounced memory deficit along with a several-fold higher load of Aβ plaques and insoluble





Aβ level, and nearly an 80-fold higher level of Aβ oligomers compared to APP/E2 mice. Oligomeric Aβ species have been shown to cause memory deficits in rodents [25] and are known for their synaptotoxic properties. This synaptotoxicity is associated with a reduction in the surface expression of various receptor proteins, including those forming the N-methyl-D-aspartate receptors [26,27], which are critical for generation of long-term potentiation in hippocampal synapses. We also found





evidence for a differential effect of apoE2 and apoE4 isoforms on Aβ metabolism in APP<sub>SW</sub>/PS1<sub>dE9</sub> mice. APP/E4 mice had significantly higher levels of soluble Aβ peptides than APP/E2 mice. In particular, the level of soluble Aβ<sub>x-42</sub>, which is considered more toxic and aggregation prone than Aβ<sub>x-40</sub>, was 22.5-fold higher in APP/E4 mice than in APP/E2 mice. Furthermore, in APP/E2 mice, the soluble Aβ<sub>x-40</sub> level was 2.1-fold higher than that of Aβ<sub>x-42</sub>, while in APP/E4 the ratio was reversed, with the level of soluble Aβ<sub>x-42</sub> being 1.4-fold higher than that of Aβ<sub>x-40</sub>. These striking differences in the brain levels of soluble Aβ<sub>x-40</sub> and Aβ<sub>x-42</sub> peptides, and the reversed ratio, between APP/E2 and APP/E4 mice are likely related to the well-established differential effect of apoE2 and apoE4 isoforms on Aβ brain clearance [28]. Increased soluble Aβ levels and a predominance of

Aβ<sub>x-42</sub> associated with the apoE4 isoform, produce a background promoting greater Aβ deposition and enhanced neurodegeneration. In fact, the load of Th-S positive Aβ plaques and the brain concentration of insoluble Aβ, which are associated with fibrillar Aβ deposits, were several-fold higher in APP/E4 mice than in APP/E2 mice. Enhanced Aβ deposition was, in turn, associated with a greater degree of neurodegeneration, as demonstrated by a several-fold higher density of neuritic plaques in APP/E4 animals as compared to APP/E2 animals. APOE ε4 targeted replacement was also associated with significantly greater co-deposition of apoE in Aβ plaques, as shown by the comparison of apoE-positive plaque load and the level of insoluble apoE between APP/E4 and APP/E2 mice. It has been previously demonstrated that co-deposition of apoE in Aβ plaques is a prerequisite for the occurrence of focal neuritic dystrophy [22,29].

Epidemiological evidence and evidence from neuropathological assessment of the impact of apoE isoforms on the brain Aβ load, have suggested that apoE2 exerts a protective effect against Aβ pathology and AD morbidity [3,9,10], while apoE4, in contrast, markedly enhances the disease process [7,8,30]. To directly examine whether apoE2 exerts a truly “therapeutic” effect or, on the contrary, is involved in promoting Aβ deposition, we systemically treated APP/E2 mice with Aβ12-28P, which disrupts the apoE/Aβ binding. Another objective of this study was to investigate whether an apoE/Aβ binding inhibitor would ameliorate Aβ pathology and associated neurodegeneration, as shown in an exaggerated form by the apoE4 isoform. We demonstrated that Aβ12-28P treatment produced significant reductions in the Aβ oligomer level, the Aβ plaque load, and the concentration of insoluble Aβ peptides, and ameliorated the neurodegenerative component of Aβ plaques in both APP/E2 and APP/E4 mice. These observations provide clear *in vivo* evidence that both apoE2 and apoE4 isoforms are involved in the process of Aβ aggregation and deposition and are associated with neurodegeneration, although the effect of apoE4 appears to be much stronger than that of apoE2. Our findings remain consistent with the effects of apoE knock-out noted in several AD Tg mouse models, where lack of apoE was associated with absence of fibrillar Aβ deposits and prevented neurodegeneration [13,29,31,32]. In addition to a marked reduction in Aβ deposition in Aβ12-28P-treated mice, we also noticed a significant reduction in the level of Aβ oligomers. It has been recently appreciated that apoE, especially its apoE4 isoform, facilitates the formation of Aβ oligomers [33,34]. Although it appears that enhanced Aβ oligomerization occurs in settings of elevated Aβ<sub>x-42</sub> level, which is associated with the apoE4 background, there is experimental evidence to indicate that direct interaction between apoE and Aβ facilitates Aβ oligomeric assembly and that all three isoforms promote

this process in the rank order  $E4 > E3 > E2$  [33]. Reduced A $\beta$  oligomer level following from disrupted apoE/A $\beta$  binding appears to provide further evidence that the direct apoE/A $\beta$  interaction enhances oligomeric assembly of A $\beta$  and that treatment with an apoE/A $\beta$  inhibitor is beneficial for preventing A $\beta$  oligomerization and for ameliorating synaptotoxicity related to A $\beta$  oligomers. Furthermore, we observed that along with reducing A $\beta$  deposition, A $\beta$ 12-28P treatment also ameliorated apoE accumulation in the brain. It has been proposed that co-deposition of apoE with A $\beta$  is an important factor promoting fibrillization of A $\beta$  and plaque formation [22,23]. It has also been recognized that co-deposition of apoE in A $\beta$  plaques promotes focal neurodegeneration in humans and in AD Tg mice [22,29,35]. Reduction of apoE deposition in A $\beta$ 12-28P-treated mice demonstrates an additional mechanism through which disruption of the apoE/A $\beta$  interaction may ameliorate A $\beta$  plaque formation and associated neurodegeneration. Similarly, it has been shown that A $\beta$  accumulation in the brain of APP<sub>SW</sub>/PS1<sub>ΔE9</sub> mice can be effectively reduced through targeting brain apoE with systemic anti-apoE passive immunization [36].

Clearance of soluble A $\beta$  from the brain is critical in preventing its accumulation and there is evidence this process can be differentially regulated by apoE isoforms [28]. Several studies have shown that the bulk of soluble A $\beta$  is cleared through its direct interaction with the LDL receptor family expressed by brain capillary endothelium [37], neurons [24,38], and astrocytes [39,40], therefore pharmacological disruption of the apoE/A $\beta$  binding is unlikely to impair this process. What is more, since some of A $\beta$  forms complexes with apoE [41], an apoE/A $\beta$  antagonist can free up this apoE bound A $\beta$  increasing soluble A $\beta$  pool and promoting its clearance. It has been also proposed that apoE can indirectly modulate A $\beta$  clearance through competing with A $\beta$  for the same receptors [40]. This notion may explain enhanced A $\beta$  clearance in the setting of apoE2, which is defective in LDL receptor binding [4,5]. Since we observed reduced levels of soluble apoE in A $\beta$ 12-28P-treated APP/E2 and APP/E4 mice, the treatment with an apoE/A $\beta$  inhibitor may additionally facilitate A $\beta$  clearance by reducing the levels of apoE competing with A $\beta$  for the same receptor clearance pathway. In fact, in our study levels of soluble A $\beta$ <sub>x-40</sub> and A $\beta$ <sub>x-42</sub> peptides were significantly reduced in both A $\beta$ 12-28P-treated APP/E2 and APP/E4 mice providing evidence that the apoE/A $\beta$  binding antagonist may enhance soluble A $\beta$  clearance.

The accumulation of A $\beta$  in the brain is considered to be a prime target of disease-modifying therapies for AD [2]. Although clinical trials of the A $\beta$ -directed mAb Bapinezumab showed no clear cognitive benefits in patients with mild to moderate AD [42], the results also indicated that APOE  $\epsilon$ 4 carrier status may limit the

response to anti-A $\beta$  passive immunization [43,44], as well as being associated with an increased rate of microbleeds and vasogenic edema [45]. As the intention of upcoming clinical trials of A $\beta$ -directed therapeutics is to target patients with early and prodromal AD [46,47], there is still a potential for differential responses to treatment among carriers of various APOE alleles. Our study provides evidence for efficacy of an agent disrupting the apoE/A $\beta$  interaction in the setting of apoE2 and apoE4 isoforms. Therefore, such an agent could be applied in human populations diversified by apoE isoform status. Furthermore, as apoE/A $\beta$  binding inhibitors would primarily target apoE promoting effect on A $\beta$  assembly and deposition, they have the potential to be combined for additive efficacy with other A $\beta$ -targeting strategies still under development, including  $\beta$ -secretase inhibitors and  $\gamma$ -secretase modulators inhibiting A $\beta$  production, or with passive immunization, which promotes A $\beta$  clearance from the brain and stimulates plaque clearance by microglia [48,49]. Results of this study justify efforts to develop clinically viable, small-molecule inhibitors of the apoE/A $\beta$  interaction and test their therapeutic application, either as a monotherapy or in conjunction with other anti-A $\beta$  approaches.

## Additional file

**Additional file 1: Detailed results concerning detection of anti-A $\beta$  antibodies, and quantification of cholesterol and apoE levels in the sera of vehicle and A $\beta$ 12-28P treated animals and detailed methods used for determination of thereof.** Demonstration of neuritic dystrophy associated with amyloid A $\beta$  plaques.

## Competing interest

JEP, MG, JK, AAA, SS, PMS have no actual or potential conflict of interest regarding the work described in this manuscript to disclose. DMH is a scientific advisor to C2N Diagnostics and is a co-inventor on US patent 7,892,845 "Methods for measuring the metabolism of neutrally derived biomolecules *in vivo*." Washington University with DMH as a co-inventor also has submitted the US non-provisional patent application "Methods for measuring the metabolism of CNS derived biomolecules *in vivo*," serial #12,267,974. DMH has consulted for Bristol-Myers Squibb, Pfizer, Satori, Innogenetics, and AstraZeneca. MJS is a co-inventor on US patents 7,632,816 "Treatment of Alzheimer Amyloid Deposits" and 8,658,677 "Pyridil-2-methylamino compounds, composition and uses thereof". New York University has also submitted with MJS as a co-inventor the US non-provisional patent application 13,134,547 "Peptoids and synthetic oligomers, pharmaceutical compositions, and methods for using same". MJS has consulted with Phillips North America and received speakers' fees from Forest Laboratories Inc. outside the submitted work.

## Acknowledgments

This work was supported by NIH/NIA awards: R01 AG31221 and K02 AG34176 to M.J.S., and R37 AG13956 to D.M.H. and by a research grant from the Stephen and Nan Swid Foundation to M.J.S.

## Author details

<sup>1</sup>Department of Neurology, New York University School of Medicine, New York, NY 10016, USA. <sup>2</sup>Department of Psychiatry, New York University School of Medicine, New York, NY 10016, USA. <sup>3</sup>Department of Biochemistry and Molecular Pharmacology, New York University School of Medicine, New York, NY 10016, USA. <sup>4</sup>Department of Neurology, Washington University School of Medicine, St. Louis, MO 63110, USA. <sup>5</sup>Knight Alzheimer's Disease Research Center, Washington University School of Medicine, St. Louis, MO 63110, USA.



<sup>6</sup>Hope Center for Neurological Disorders, Washington University School of Medicine, St. Louis, MO 63110, USA. <sup>7</sup>Department of Neuroscience, Mayo Clinic College of Medicine, Jacksonville, FL 32224, USA. <sup>8</sup>Department of Medicine (Geriatrics), Duke University School of Medicine, Durham, NC 27710, USA. <sup>9</sup>Durham VA Medical Center's Geriatric Research, Education, and Clinical Center, Durham, NC 27710, USA. <sup>10</sup>New York University School of Medicine, Alexandria East River Science Park, 450E 29th St., Room 830, New York, NY 10016, USA.

Received: 16 June 2014 Accepted: 16 June 2014

Published online: 28 June 2014

## References

1. Querfurth HW, LaFerla FM (2010) Alzheimer's disease. *N Engl J Med* 362(4):329–344
2. Selkoe DJ (2011) Resolving controversies on the path to Alzheimer's therapeutics. *Nat Med* 17(9):1060–1065
3. Liu CC, Kanekiyo T, Xu H, Bu G (2013) Apolipoprotein E and Alzheimer disease: risk, mechanisms and therapy. *Nat Rev Neurol* 9(2):106–118
4. Mahley RW, Weisgraber KH, Huang Y (2009) Apolipoprotein E: structure determines function, from atherosclerosis to Alzheimer's disease to AIDS. *J Lipid Res* 50 Suppl:S183–S188
5. Wilson C, Wardell MR, Weisgraber KH, Mahley RW, Agard DA (1991) Three-dimensional structure of the LDL receptor-binding domain of human apolipoprotein E. *Science* 252(5014):1817–1822
6. Corder EH, Saunders AM, Strittmatter WJ, Schmechel DE, Gaskell PC Jr, Rimmer JB, Locke PA, Conneally PM, Schmechel KE, Tanzi RE, Gusella JF, Small GW, Roses AD, Pericak-Vance MA, Haines JL (1995) Apolipoprotein E, survival in Alzheimer's disease patients, and the competing risks of death and Alzheimer's disease. *Neurology* 45(7):1323–1328
7. Corder EH, Saunders AM, Strittmatter WJ, Schmechel DE, Gaskell PC, Small GW, Roses AD, Haines JL, Pericak-Vance MA (1993) Gene dose of apolipoprotein E type 4 allele and the risk of Alzheimer's disease in late onset families. *Science* 261(5123):921–923
8. Strittmatter W, Roses A (1996) Apolipoprotein E and Alzheimer's disease. *Annu Rev Neurosci* 19:53–77
9. Corder EH, Saunders AM, Risch NJ, Strittmatter WJ, Schmechel DE, Gaskell PC Jr, Rimmer JB, Locke PA, Conneally PM, Schmechel KE, Small GW, Roses AD, Haines JL, Pericak-Vance MA (1994) Protective effect of apolipoprotein E type 2 allele for late onset Alzheimer disease. *Nat Genet* 7(2):180–184
10. West HL, Rebeck GW, Hyman BT (1994) Frequency of the apolipoprotein E epsilon 2 allele is diminished in sporadic Alzheimer disease. *Neurosci Lett* 175(1–2):46–48
11. Ma J, Brewer BH, Potter H, Brewer HB Jr (1996) Alzheimer Ab neurotoxicity: promotion by antichymotrypsin, apoE4; inhibition by Ab-related peptides. *Neurobiol Aging* 17:773–780
12. Sadowski M, Pankiewicz J, Scholtzova H, Ripellino JA, Li YS, Schmidt SD, Mathews PM, Fryer JD, Holtzman DM, Sigurdsson EM, Wisniewski T (2004) A synthetic peptide blocking the apolipoprotein E/beta-amyloid binding mitigates beta-amyloid toxicity and fibril formation *in vitro* and reduces beta-amyloid plaques in transgenic mice. *Am J Pathol* 165(3):937–948
13. Kuszczuk MA, Sanchez S, Pankiewicz J, Kim J, Duszczyk M, Guridi M, Asuni AA, Sullivan PM, Holtzman DM, Sadowski MJ (2013) Blocking the interaction between apolipoprotein E and abeta reduces intraneuronal accumulation of abeta and inhibits synaptic degeneration. *Am J Pathol* 182(5):1750–1768
14. Garcia-Alloza M, Robbins EM, Zhang-Nunes SX, Purcell SM, Betensky RA, Raju S, Prada C, Greenberg SM, Bacskai BJ, Frosch MP (2006) Characterization of amyloid deposition in the APPsw/PS1dE9 mouse model of Alzheimer disease. *Neurobiol Dis* 24(3):516–524
15. Sadowski MJ, Pankiewicz J, Scholtzova H, Mehta PD, Prelli F, Quartermain D, Wisniewski T (2006) Blocking the apolipoprotein E/amyloid-beta interaction as a potential therapeutic approach for Alzheimer's disease. *Proc Natl Acad Sci U S A* 103(49):18787–18792
16. Knouff C, Hinsdale ME, Mezdour H, Altenburg MK, Watanabe M, Quarfordt SH, Sullivan PM, Maeda N (1999) Apo E structure determines VLDL clearance and atherosclerosis risk in mice. *J Clin Invest* 103(11):1579–1586
17. Sullivan PM, Mezdour H, Quarfordt SH, Maeda N (1998) Type III hyperlipoproteinemia and spontaneous atherosclerosis in mice resulting from gene replacement of mouse Apoe with human Apoe\*2. *J Clin Invest* 102(1):130–135
18. Sullivan PM, Mezdour H, Aratani Y, Knouff C, Najib J, Reddick RL, Quarfordt SH, Maeda N (1997) Targeted replacement of the mouse apolipoprotein E gene with the common human APOE3 allele enhances diet-induced hypercholesterolemia and atherosclerosis. *J Biol Chem* 272(29):17972–17980
19. Asuni AA, Guridi M, Pankiewicz JE, Sanchez S, Sadowski MJ (2014) Modulation of amyloid precursor protein expression reduces beta-amyloid deposition in a mouse model. *Ann Neurol* 75(5):684–699
20. Dodart JC, Bales KR, Gannon KS, Greene SJ, DeMattos RB, Mathis C, DeLong CA, Wu S, Wu X, Holtzman DM, Paul SM (2002) Immunization reverses memory deficits without reducing brain A beta burden in Alzheimer's disease model. *Nat Neurosci* 5(5):452–457
21. Braak H, Braak E (1991) Neuropathological staging of Alzheimer-related changes. *Acta Neuropathol* 82:239–259
22. Wisniewski HM, Sadowski M, Jakubowska-Sadowska K, Tarnawski M, Wegiel J (1998) Diffuse, lake-like amyloid-beta deposits in the paraventricular layer of the presubiculum in Alzheimer disease. *J Neuropathol Exp Neurol* 57(7):674–683
23. Wisniewski T, Lalowski M, Golabek AA, Vogel T, Frangione B (1995) Is Alzheimer's disease an apolipoprotein E amyloidosis? *Lancet* 345(8955):956–958
24. Kim J, Castellano JM, Jiang H, Basak JM, Parsadanian M, Pham V, Mason SM, Paul SM, Holtzman DM (2009) Overexpression of low-density lipoprotein receptor in the brain markedly inhibits amyloid deposition and increases extracellular A beta clearance. *Neuron* 64(5):632–644
25. Shankar GM, Li S, Mehta TH, Garcia-Munoz A, Shepardson NE, Smith I, Brett FM, Farrell MA, Rowan MJ, Lemere CA, Regan CM, Walsh DM, Sabatini BL, Selkoe DJ (2008) Amyloid-beta protein dimers isolated directly from Alzheimer's brains impair synaptic plasticity and memory. *Nat Med* 14(8):837–842
26. Shankar GM, Bloodgood BL, Townsend M, Walsh DM, Selkoe DJ, Sabatini BL (2007) Natural oligomers of the Alzheimer amyloid-beta protein induce reversible synapse loss by modulating an NMDA-type glutamate receptor-dependent signaling pathway. *J Neurosci* 27(11):2866–2875
27. Snyder EM, Nong Y, Almeida CG, Paul S, Moran T, Choi EY, Nairn AC, Salter MW, Lombroso PJ, Gouras GK, Greengard P (2005) Regulation of NMDA receptor trafficking by amyloid-beta. *Nat Neurosci* 8(8):1051–1058
28. Castellano JM, Kim J, Stewart FR, Jiang H, DeMattos RB, Patterson BW, Fagan AM, Morris JC, Mawuenyega KG, Cruchaga C, Goate AM, Bales KR, Paul SM, Bateman RJ, Holtzman DM (2011) Human apoE isoforms differentially regulate brain amyloid-beta peptide clearance. *Sci Transl Med* 3(89):89ra57
29. Holtzman DM, Bales KR, Tenkova T, Fagan AM, Parsadanian M, Sartorius LJ, Mackey B, Olney J, McKeel D, Wozniak D, Paul SM (2000) Apolipoprotein E isoform-dependent amyloid deposition and neuritic degeneration in a mouse model of Alzheimer's disease. *Proc Natl Acad Sci U S A* 97:2892–2897
30. Hudry E, Dashkoff J, Roe AD, Takeda S, Koffie RM, Hashimoto T, Scheel M, Spire-Jones T, rbel-Ornath M, Betensky R, Davidson BL, Hyman BT (2013) Gene transfer of human apoE isoforms results in differential modulation of amyloid deposition and neurotoxicity in mouse brain. *Sci Transl Med* 5(212):212ra161
31. Bales KR, Verina T, Dodel RC, Du YS, Altstiel L, Bender M, Hyslop P, Johnstone EM, Little SP, Cummins DJ, Piccardo P, Ghetti B, Paul SM (1997) Lack of apolipoprotein E dramatically reduces amyloid b-peptide deposition. *Nat Genet* 17(3):263–264
32. Fryer JD, Taylor JW, DeMattos RB, Bales KR, Paul SM, Parsadanian M, Holtzman DM (2003) Apolipoprotein E markedly facilitates age-dependent cerebral amyloid angiopathy and spontaneous hemorrhage in amyloid precursor protein transgenic mice. *J Neurosci* 23(21):7889–7896
33. Hashimoto T, Serrano-Pozo A, Hori Y, Adams KW, Takeda S, Banerji AO, Mitani A, Joyner D, Thyssen DH, Bacskai BJ, Frosch MP, Spire-Jones TL, Finn MB, Holtzman DM, Hyman BT (2012) Apolipoprotein E, especially apolipoprotein E4, increases the oligomerization of amyloid beta peptide. *J Neurosci* 32(43):15181–15192
34. Koffie RM, Hashimoto T, Tai HC, Kay KR, Serrano-Pozo A, Joyner D, Hou S, Kopeikina KJ, Frosch MP, Lee VM, Holtzman DM, Hyman BT, Spire-Jones TL (2012) Apolipoprotein E4 effects in Alzheimer's disease are mediated by synaptotoxic oligomeric amyloid-beta. *Brain* 135(Pt 7):2155–2168
35. Marques MA, Owens PA, Crutcher KA (2004) Progress toward identification of protease activity involved in proteolysis of apolipoprotein e in human brain. *J Mol Neurosci* 24(1):73–80
36. Kim J, Eitorai AE, Jiang H, Liao F, Verghese PB, Kim J, Stewart FR, Basak JM, Holtzman DM (2012) Anti-apoE immunotherapy inhibits amyloid accumulation in a transgenic mouse model of Abeta amyloidosis. *J Exp Med* 209(12):2149–2156
37. Deane R, Wu ZH, Sagare A, Davis J, Yan SD, Hamm K, Xu F, Parisi M, Larue B, Hu HW, Spijkers P, Guo H, Song XM, Lenting PJ, van Nostrand WE, Zlokovic

- BV (2004) LRP/amyloid beta-peptide interaction mediates differential brain efflux of A beta isoforms. *Neuron* 43(3):333–344
38. Kanekiyo T, Cirrito JR, Liu CC, Shinohara M, Li J, Schuler DR, Shinohara M, Holtzman DM, Bu G (2013) Neuronal clearance of amyloid-beta by endocytic receptor LRP1. *J Neurosci* 33(49):19276–19283
39. Basak JM, Verghese PB, Yoon H, Kim J, Holtzman DM (2012) Low-density lipoprotein receptor represents an apolipoprotein E-independent pathway of Abeta uptake and degradation by astrocytes. *J Biol Chem* 287(17):13959–13971
40. Verghese PB, Castellano JM, Garai K, Wang Y, Jiang H, Shah A, Bu G, Frieden C, Holtzman DM (2013) ApoE influences amyloid-beta (Abeta) clearance despite minimal apoE/Abeta association in physiological conditions. *Proc Natl Acad Sci U S A* 110(19):E1807–E1816
41. Tai LM, Mehra S, Shete V, Estus S, Rebeck GW, Bu G, LaDu MJ (2014) Soluble apoE/Abeta complex: mechanism and therapeutic target for APOE4-induced AD risk. *Mol Neurodegener* 9:2
42. Tayeb HO, Murray ED, Price BH, Tarazi FI (2013) Bapineuzumab and solanezumab for Alzheimer's disease: is the 'amyloid cascade hypothesis' still alive? *Expert Opin Biol Ther* 13(7):1075–1084
43. Kaufer D, Gandy S (2009) APOE ε4 and bapineuzumab: infusing pharmacogenomics into Alzheimer disease therapeutics. *Neurology* 73(24):2052–2053
44. Salloway S, Sperling R, Gilman S, Fox NC, Blennow K, Raskind M, Sabbagh M, Honig LS, Doody R, Van Dyck CH, Mulnard R, Barakos J, Gregg KM, Liu E, Lieberburg I, Schenk D, Black R, Grundman M (2009) A phase 2 multiple ascending dose trial of bapineuzumab in mild to moderate Alzheimer disease. *Neurology* 73(24):2061–2070
45. Sperling RA, Jack CR Jr, Black SE, Frosch MP, Greenberg SM, Hyman BT, Scheltens P, Carrillo MC, Thies W, Bednar MM, Black RS, Brashear HR, Grundman M, Siemers ER, Feldman HH, Schindler RJ (2011) Amyloid-related imaging abnormalities in amyloid-modifying therapeutic trials: recommendations from the Alzheimer's Association Research Roundtable Workgroup. *Alzheimers Dement* 7(4):367–385
46. Lambracht-Washington D, Rosenberg RN (2013) Advances in the development of vaccines for Alzheimer's disease. *Discov Med* 15(84):319–326
47. Lemere CA (2013) Immunotherapy for Alzheimer's disease: hoops and hurdles. *Mol Neurodegener* 8(1):36
48. DeMattos RB, Bales KR, Cummins DJ, Dodart JC, Paul SM, Holtzman DM (2001) Peripheral anti-A beta antibody alters CNS and plasma A beta clearance and decreases brain A beta burden in a mouse model of Alzheimer's disease. *Proc Natl Acad Sci U S A* 98(15):8850–8855
49. Ostrowitzki S, Deptula D, Thurjell L, Barkhof F, Bohrmann B, Brooks DJ, Klunk WE, Ashford E, Yoo K, Xu ZX, Loetscher H, Santarelli L (2012) Mechanism of amyloid removal in patients with Alzheimer disease treated with gantenerumab. *Arch Neurol* 69(2):198–207

doi:10.1186/s40478-014-0075-0

**Cite this article as:** Pankiewicz et al.: Blocking the apoE/Aβ interaction ameliorates Aβ-related pathology in APOE ε2 and ε4 targeted replacement Alzheimer model mice. *Acta Neuropathologica Communications* 2014 **2**:75.

**Submit your next manuscript to BioMed Central  
and take full advantage of:**

- Convenient online submission
- Thorough peer review
- No space constraints or color figure charges
- Immediate publication on acceptance
- Inclusion in PubMed, CAS, Scopus and Google Scholar
- Research which is freely available for redistribution

Submit your manuscript at  
www.biomedcentral.com/submit

